Proceedings of the 8th International Conference on Energy Harvesting, Storage, and Transfer (EHST 2025)
July 15, 2025 - July 17, 2025 | Imperial College London Conference, London, United Kingdom
Paper No. 137
DOI: 10.11159/ehst25.137

A Triboelectric-Based Wearable Platform for Early Flatfoot Detection

Mohammad Alghamaz[1], Leila Donyaparastlivari[1], Alwathiqbellah Ibrahim[1,*], and Nelson Fumo[1]
The University of Texas at Tyler
3900 University Blvd., Tyler, Texas 75799
malghamaz@patriots.uttyler.edu; ldonyaparastlivari@patriots.uttyler.edu;
aibrahim@uttyler.edu; nfumo@uttyler.edu

Abstract **-** This study presents a self-powered smart insole designed for continuous foot health monitoring, with a specific focus on early flatfoot detection. The insole incorporates triboelectric energy harvesters positioned at key plantar regions to convert ground reaction forces during walking into measurable electrical signals. In proof-of-concept trials involving a single participant, flatfoot was simulated by reducing the medial arch height by 70%. In the healthy-foot condition, the medial arch sensor produced minimal output, while the simulated flatfoot condition generated a significantly higher voltage. These findings validate the insole's capability to differentiate between normal and collapsed arches in real time, underscoring its potential for early diagnosis, personalized rehabilitation, and preventive foot care.

Keywords**:** Triboelectric, Energy harvesting; Flatfoot, Health Monitoring, Smart Insole
*Corresponding author: Alwathiqbellah Ibrahim, aibrahim@uttyler.edu

1. Introduction

The human foot is our primary interface with the ground, dissipating impact forces and providing critical sensory feedback for steady, efficient walking [1]. During gait, each step generates a vertical ground reaction force (GRF), the magnitude and timing of which depend on body mass, walking speed, and foot-ground contact area [2,3]. Beyond structural support, plantar receptors transmit sensory input to the central nervous system, enabling rapid adjustments in posture and stride on irregular surfaces.

Pes planus, or flatfoot, occurs when the medial arch collapses, either through flexible soft tissue elongation or rigid structural deformation [4,5]. Although often painless in childhood, symptomatic flatfoot can lead to chronic joint discomfort, muscular fatigue, stress fractures, and a cascade of lower-limb overuse injuries [6,7]. By altering the normal inward and outward rolling cycle, arch collapse shifts the load laterally, increases calcaneal eversion, and reduces propulsive efficiency during the mid- to late-stance phases of walking. These biomechanical disruptions impair gait economy and elevate the risk of secondary issues such as posterior tibial tendon dysfunction and patellofemoral joint pain [8,9].

Conventional diagnostic methods including pedobarographic analysis [10], footprint assessment [11], baropodometric evaluation [12,13], and radiographic imaging offer valuable snapshots of arch morphology but require clinical settings, specialized equipment, and provide only intermittent data [14–16]. Such episodic assessments can miss early arch collapse and fail to support continuous monitoring in real-world conditions. A wearable device capable of continuously recording foot mechanics during everyday walking could transform flatfoot management by enabling early detection and timely intervention before symptoms develop.

Triboelectric transduction is a widely used energy-harvesting mechanism due to its simplicity, affordability, and ability to generate electricity from routine mechanical motions [17]. A key advantage is its direct proportionality between the applied mechanical load and the resulting electrical signal, enabling both efficient energy conversion and accurate force sensing [18, 19]. These features make triboelectric systems highly suitable for self-powered wearable devices, where energy harvesting and biomechanical monitoring are both essential.

In this feasibility study, we introduce a self-powered smart insole that employs triboelectric energy harvesters placed at the heel, lateral arch, and medial arch to convert walking-induced GRFs into quantifiable electrical outputs. During proof-of-concept trials with a single volunteer, flatfoot was simulated by reducing the medial arch height by 70 percent. Under normal gait conditions, the medial arch sensor produced minimal output, indicating limited ground contact. In contrast, the simulated flatfoot condition generated a distinct voltage surge, directly linking arch collapse to electrical activity. This low-cost, continuously operating platform provides real-time feedback on arch integrity, laying the foundation for early diagnosis, personalized rehabilitation, and proactive flatfoot management.

2. Harvester Design and Working Principle:

Figure 1 presents the design and internal structure of the triboelectric harvesters embedded within the smart insole. Panel (a) shows the strategic placement of the harvesters beneath the metatarsals, lateral arch, medial arch, and heel. These locations were selected to capture a spatially distributed profile of ground reaction forces (GRFs) throughout the gait cycle, which is critical for detecting localized pressure changes associated with flatfoot. Panels (b) and (c) illustrate the harvester's operational states during walking. In the separation mode (b), the layers remain apart under no load, while in the contact mode (c), compressive forces from foot strikes bring the layers together, enabling charge generation through triboelectric interaction. Panel (d) provides an exploded view of the harvester, showing its main components: the moving electrode, fixed electrode, PDMS dielectric layer, and the spring elements responsible for restoring the separation after contact. To enhance user comfort and eliminate the need for exposed hardware, panel (e) demonstrates how mechanical springs are anchored into precision-engineered grooves within the housing. This groove-based assembly ensures stable operation, maintains structural integrity, and preserves a smooth and comfortable surface for continuous wear.

The integration of multiple identical triboelectric harvesters in geometry and materials that converts walking-induced ground reaction forces (GRFs) into proportional electrical signals will ensure that any differences in output voltages are due to actual variations in local GRFs rather than inconsistencies in design. This uniformity enhances the accuracy and reliability of early flatfoot detection.

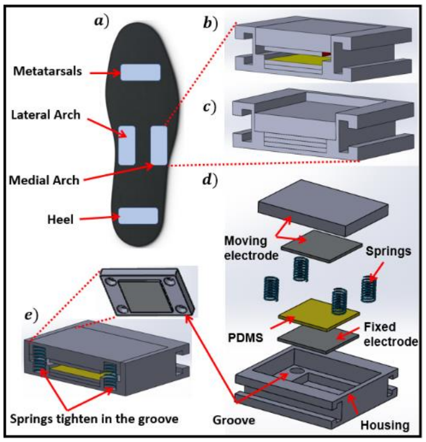

Figure 1:(a) Design of the integrated triboelectric harvesters in the insole at the Metatarsals, Lateral Arch, Medial Arch, and Heel positions, (b) Compact triboelectric generator at the separation mode, (c) Compact triboelectric generator at the contact mode, (d)Take-off components of the triboelectric generator, (e) Mechanical Springs tighten inside the grooves.

Daily walking imparts vertical ground reaction forces (GRFs) to the foot. These forces not only contribute to potential arch collapse but also represent a valuable source of recoverable mechanical energy. To capture and monitor these loads, we embedded four identical triboelectric harvesters into a commercial insole at the metatarsals, medial arch, lateral arch, and heel. Each harvester consists of two aluminium electrodes bonded to a PDMS dielectric layer, with compression springs maintaining a 0.5 to 1 cm gap to enable the repeated contact and separation motion essential for triboelectric conversion. By standardizing the harvester geometry and materials, any variations in output voltage reflect actual differences in local GRFs rather than design inconsistencies. The screw-free, grooved housings securely anchor the springs without protrusions, preserving foot comfort during prolonged use. Designed to withstand thousands of walking cycles, the insole can be inserted into standard footwear to provide continuous, real-time monitoring of arch integrity.

The triboelectric generator operates through a repeated cycle of contact and separation between the aluminium and PDMS layers, driven by GRFs during walking. When compressed, the layers come into contact, generating opposite charges due to their differing electron affinities. As the foot lifts and the layers separate, a potential difference develops, causing current to flow. With each subsequent step, the cycle reverses, producing current in the opposite direction. This continuous contact–separation process generates alternating current, allowing the system to perform both force sensing and energy harvesting during natural gait. As a result, the smart insole functions as a self-powered health monitoring device, where increased electrical output from the medial arch harvester, relative to the others, can indicate the presence and severity of flatfoot conditions.

3. Experimental Setup:

The experimental setup for evaluating the smart insole under walking conditions is shown in Figure 2. A participant walked on a treadmill at a constant speed of 3 mph, as shown in Figure 2a. Each triboelectric harvester embedded in the insole was connected to a separate oscilloscope channel to capture the corresponding electrical output signals in real time, as illustrated in Figure 2b.

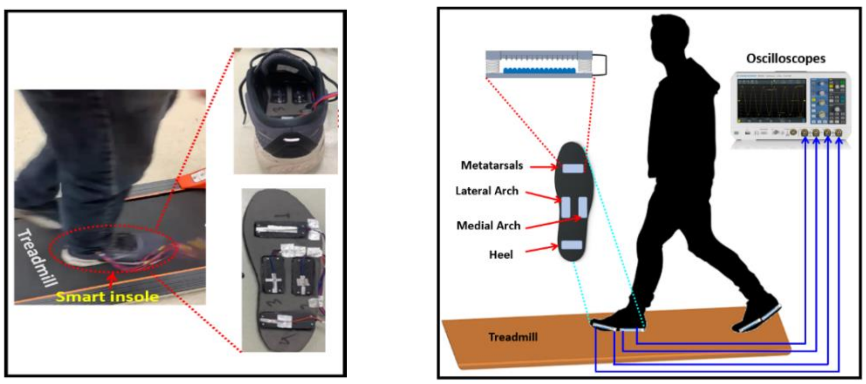

(a) (b)

Figure 2: The experimental setup used for testing: (a) The shoe with smart insole including the fabricated triboelectric harvesters, (b) Schematic for the experimental setup.

A proof-of-concept evaluation was conducted with a single participant under two walking conditions: intact arch and simulated flatfoot. This approach was used to establish a baseline and assess changes in foot mechanics. In the simulated flatfoot condition, a 3D-printed spacer was used to reduce the medial arch height by approximately 70 percent, enabling a direct comparison of the insole's electrical responses between normal and collapsed arch states. The participant walked on a treadmill at a constant speed of 3 mph, while each of the four embedded triboelectric harvesters was connected to a separate oscilloscope channel to record voltage outputs in real time. To ensure data reliability, each condition was tested in triplicate, isolating the effects of arch deformation on sensor output and demonstrating the device's capability for early flatfoot detection.

4. Results and Discussion:

Under controlled walking trials at 3 mph, we compared the voltage outputs from the four triboelectric harvesters located at the metatarsals, lateral arch, medial arch, and heel under both normal and simulated flatfoot conditions. In the healthy-arch trials, the medial arch sensor generated low voltage output, while the metatarsal and heel sensors produced significantly higher signals, consistent with normal load distribution. Under the flatfoot condition, however, the medial arch voltage increased markedly, reflecting greater ground contact in that region. In contrast, the metatarsal and heel signals showed only minor changes. These location-specific variations demonstrate the insole's ability to detect localized shifts in plantar loading and its effectiveness in continuously monitoring arch support in real time.

4.1. Normal Foot:

Figure 3 summarizes three walking trials conducted at a speed of 3 mph. Panels (a), (c), and (e) display the time-domain voltage traces recorded from the metatarsal, lateral arch, medial arch, and heel sensors, while the corresponding RMS bar charts in panels (b), (d), and (f) illustrate their average signal amplitudes. Across all trials, the insole demonstrated excellent repeatability, with nearly identical signal magnitudes at each sensor location. As expected for a healthy foot, the medial arch sensor consistently produced the lowest RMS voltage, reflecting minimal plantar contact and reduced ground reaction forces. In contrast, the metatarsal and heel sensors exhibited higher but stable outputs. These findings confirm the smart insole's capability to resolve localized load distribution during walking and establish a reliable baseline for comparison with flatfoot conditions.

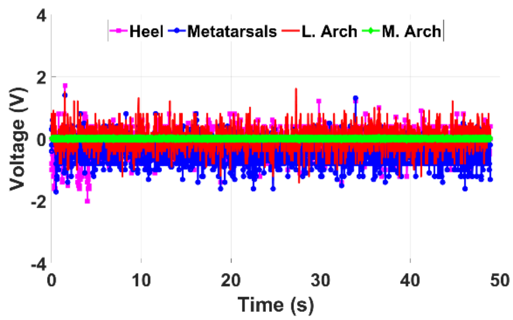

(a)

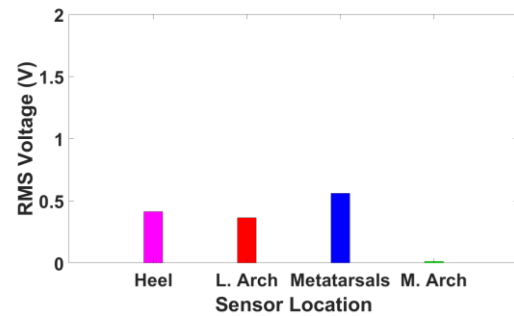

(b)

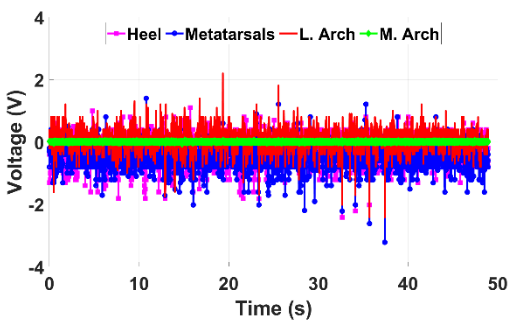

(c)

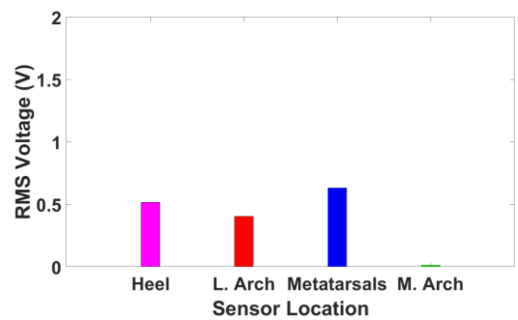

(d)

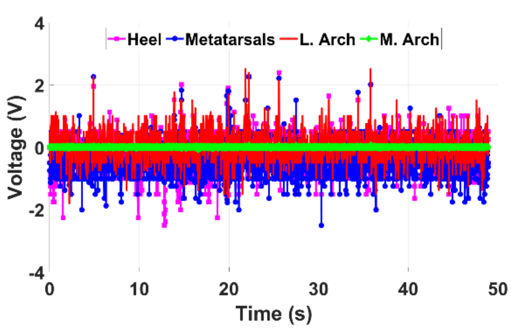

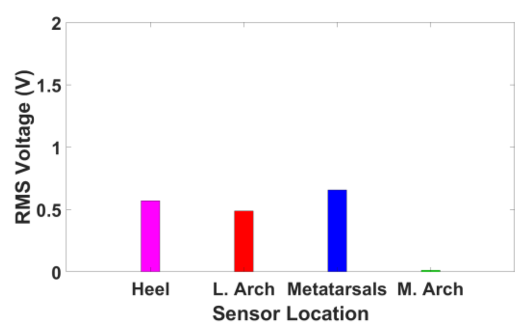

(e) (f)

Figure 3: Time-domain voltage signals generated during three walking trials, shown in panels (a), (c), and (e), with their corresponding root mean square (RMS) values presented as bar plots in panels (b), (d), and (f).

Figure 4 summarizes the insole's performance across three walking trials at 3 mph by presenting the mean RMS voltage values recorded at each harvester location: 0.499 V at the metatarsals, 0.419 V at the lateral arch, 0.616 V at the medial arch, and 0.013 V at the heel. The notably low output from the medial arch sensor aligns with the expected minimal loading in that region for a healthy foot. In contrast, the higher voltage readings at the metatarsals and lateral arch correspond to the primary weight-bearing areas during the mid-stance and toe-off phases of walking.

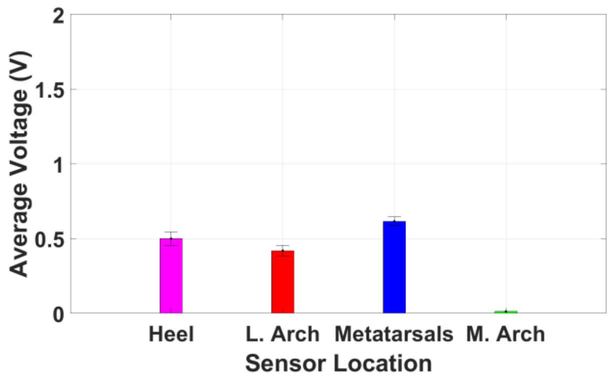

Figure 4: Average voltage outputs from three walking trials, illustrating the mean electrical signals recorded from each sensor during the walking activity.

Intertrial variability, as measured by standard deviations of 0.0797 V, 0.0635 V, 0.0502 V, and 0.0007 V across the metatarsals, lateral arch, medial arch, and heel respectively, remained low for all sensor locations. The medial arch sensor again demonstrated exceptional stability with a standard deviation of just 0.0007 V. Corresponding standard error values of 0.0460 V, 0.0367 V, 0.0290 V, and 0.0004 V further highlight the precision of these measurements. These consistently low variances and errors confirm the smart insole's ability to reliably capture localized ground reaction forces during walking, providing a strong and repeatable baseline for detecting the subtle loading changes associated with early flatfoot development.

4.2 Flatfoot Condition:

A flatfoot evaluation was conducted using the same participant walking on a treadmill at 3 mph. In this trial, a 3D-printed PLA insert was placed beneath the medial arch to reduce its height by approximately 70 percent, as shown in Figure 5. Each of the four embedded triboelectric harvesters, located at the metatarsals, lateral arch, medial arch, and heel, was connected to its own oscilloscope channel to capture voltage outputs in real time. Three walking trials were performed in triplicate under the simulated flatfoot condition, following the same protocol used for the healthy-foot assessment. This setup allowed for clear isolation of the effects of medial arch collapse on the electrical signals and demonstrated the insole's sensitivity and effectiveness when medial arch support is compromised.

produced a distinct voltage waveform at the medial arch. The RMS amplitude rose well above its baseline noise level, indicating increased ground contact. Meanwhile, the metatarsal and heel sensors maintained their characteristic profiles, suggesting that the altered loading was localized to the collapsed arch region. This pronounced response at the medial arch confirms the smart insole's ability to detect biomechanical changes associated with flatfoot and demonstrates its effectiveness for continuous monitoring of arch integrity in real time.

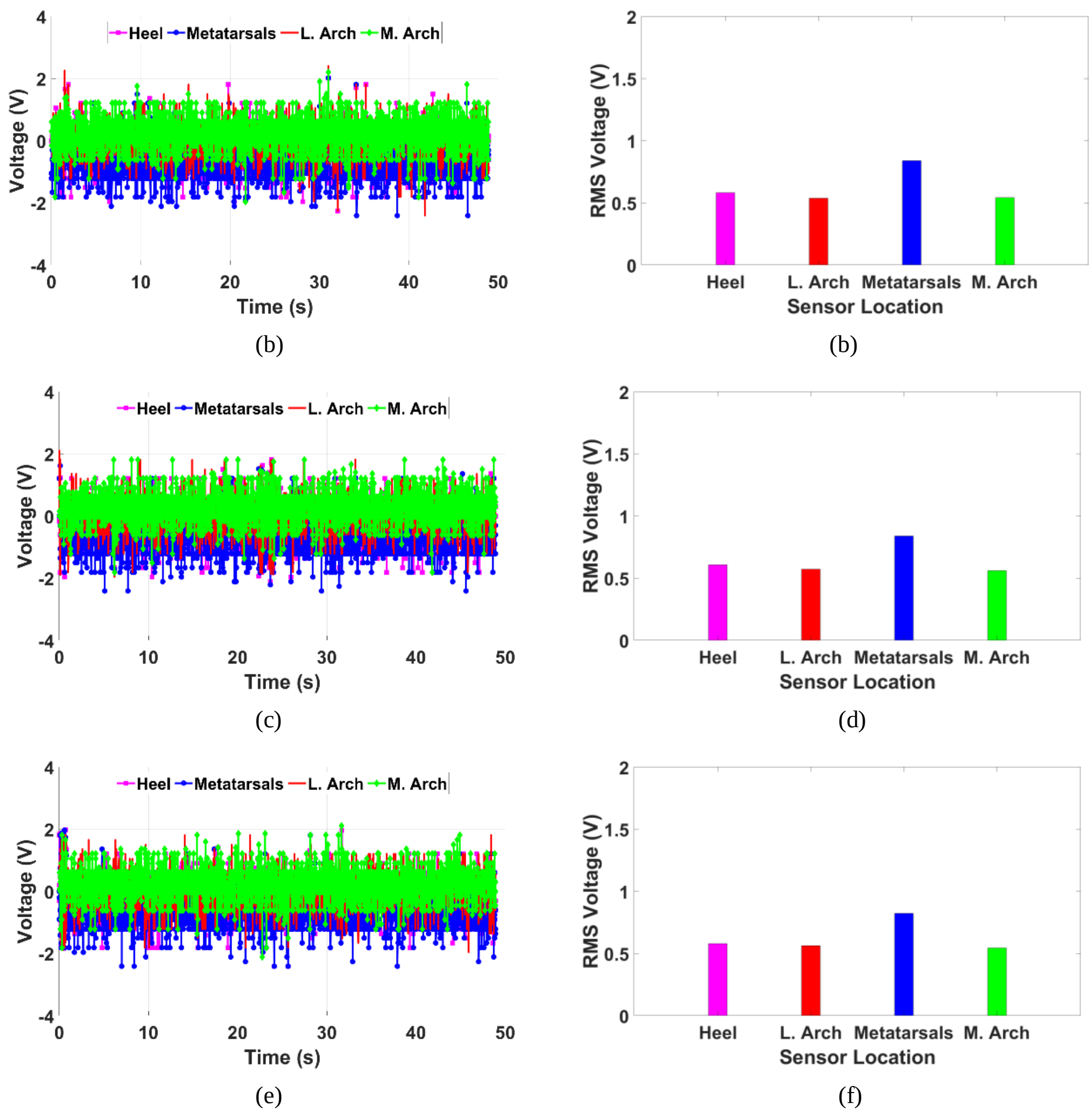

Figure 6: The generated electrical signals for three different walking activity measurements in time response (a, c, e) alongside their corresponding root mean square (RMS) electrical signals depicted as bar plots (b, d, f), from the unhealthy foot.

During 3 mph walking with the medial arch reduced by approximately 70 percent, the mean RMS voltages at each sensor location shifted as follows: metatarsals at approximately 0.590 V, lateral arch at 0.558 V, medial arch at 0.549 V, and heel at 0.834 V, as shown in Figure 8. Notably, the medial arch sensor, which previously showed near-zero output during healthy trials, now produced a clear signal of approximately 0.55 V. This confirms increased ground contact resulting from arch collapse, although the medial arch still exhibited the lowest voltage among all sites due to the partial nature of the deformation. This graded response, where larger structural deformation results in higher voltage output, indicates that the smart insole is capable not only of detecting flatfoot but also of quantifying its severity. Low variability across trials further demonstrates the system's reliability for continuous and real-time monitoring of arch integrity. Standard deviations of 0.0159, 0.0172, 0.0094, and 0.0109 for the metatarsals, lateral arch, medial arch, and heel, respectively, reflect stable sensor performance, with slightly higher fluctuation at the medial arch due to loading inconsistencies. Corresponding standard error values ranging from 0.0092 to 0.0063 confirm the precision and consistency of the measurements across repeated trials. These results validate the smart insole's ability to reliably capture changes associated with foot arch deformation, supporting its application as a diagnostic tool for early detection and continuous monitoring of flatfoot progression.

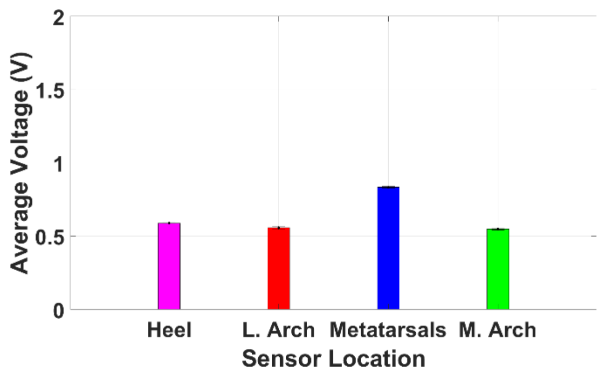

Figure 8: The average voltage from three different walking activity measurements.

The results of this feasibility study highlight the effectiveness of triboelectric sensing as a quantitative method for assessing localized plantar load distribution. The smart insole consistently captured voltage variations associated with medial arch deformation, demonstrating its potential as an embedded diagnostic tool for early flatfoot detection. Its self-powered operation, standardized harvester design, and high signal reliability across trials present a promising foundation for future clinical implementation and integration into advanced gait analysis systems.

5. Conclusion:

This proof-of-concept study demonstrated a self-powered smart insole capable of real-time foot health monitoring during walking. In controlled trials at a walking speed of 3 mph, the insole's four triboelectric harvesters, positioned at the metatarsals, lateral arch, medial arch, and heel, consistently converted ground reaction forces into proportional voltage signals. Under healthy-foot conditions, the medial arch sensor showed minimal output, while the metatarsal and heel sensors exhibited their expected signal patterns. When flatfoot was simulated by reducing the medial arch height by 70 percent using a 3D-printed insert, the medial arch sensor produced a noticeable voltage increase, although still lower than the other sites due to partial arch deformation. High repeatability across triplicate trials and low intertrial variability confirmed the system's reliability for continuous monitoring. The observed graded voltage response to arch deformation underscores the insole's capability not only to detect the presence of flatfoot but also to quantify its severity. These findings support the smart insole's potential for future wearable systems designed to enable early intervention and personalized rehabilitation.

6. References:

[1] R. Riemer and A. Shapiro, "Biomechanical energy harvesting from human motion: theory, state of the art, design guidelines, and future directions," *J. NeuroEngineering Rehabil.*, vol. 8, pp. 1–13, 2011.

[2] S. Morrison, M. Tait, E. Bong, K. Kane, and C. Nester, "Symptomatic pes planus in children: a synthesis of allied health professional practices," *J. Foot Ankle Res.*, vol. 13, pp. 1–7, 2020.

[3] M. Alghamaz, L. Donyaparastlivari, and A. Ibrahim, "Dynamic response and energy conversion of coupled cantilevers with dual piezoelectric–triboelectric harvesting mechanisms," *Micromachines*, vol. 16, no. 2, p. 182, 2025.[4] K. Kaufman, S. Brodine, R. Shaffer, C. Johnson, and T. Cullison, "The effect of foot structure and range of motion on musculoskeletal overuse injuries," *Am. J. Sports Med.*, vol. 27, pp. 585–593, 1999.

[4] K. Kaufman, S. Brodine, R. Shaffer, C. Johnson, and T. Cullison, "The effect of foot structure and range of motion on musculoskeletal overuse injuries," *Am. J. Sports Med.*, vol. 27, pp. 585–593, 1999.

[5] Y. Chen, S. Lou, C. Huang, and F. Su, "Effects of foot orthoses on gait patterns of flat feet patients," *Clin. Biomech.*, vol. 25, pp. 265–270, 2010.

[6] P. Levinger, G. Murley, C. Barton, M. Cotchett, S. McSweeney, and H. Menz, "A comparison of foot kinematics in people with normal- and flat-arched feet using the Oxford foot model," *Gait Posture*, vol. 32, pp. 519–523, 2010.

[7] Chang, C.H., Chen, Y.C., Yang, W.T., Ho, P.C., Hwang, A.W., Chen, C.H., Chang, J.H. and Chang, L.W., 2014. Flatfoot diagnosis by a unique bimodal distribution of footprint index in children. PLoS One, 9(12), p.e115808.

[8] M. Hosl, H. Böhm, C. Multerer, and L. Döderlein, "Does excessive flatfoot deformity affect function? A comparison between symptomatic and asymptomatic flatfeet using the Oxford foot model," *Gait Posture*, vol. 39, pp. 23–28, 2014.

[9] Y. Huang, H. Peng, X. Wang, Z. Chen, and C. Song, "The arch support insoles show benefits to people with flatfoot on stance time, cadence, plantar pressure and contact area," *PLoS One*, vol. 15, p. e0237382, 2020.

[10] Pita-Fernández, S., González-Martín, C., Seoane-Pillado, T., López-Calviño, B., Pértega-Díaz, S. and Gil-Guillén, V., 2015. Validity of footprint analysis to determine flatfoot using clinical diagnosis as the gold standard in a random sample aged 40 years and older. Journal of epidemiology, 25(2), pp.148-154.

[11] P. Igbigbi and B. Msamati, "The footprint ratio as a predictor of pes planus: A study of indigenous Malawians," *J. Foot Ankle Surg.*, vol. 41, pp. 394–397, 2002.

[12] G. Troiano, N. Nante, and G. Citarelli, "Pes planus and pes cavus in southern," *Ann. Ist. Super. Sanità*, vol. 53, pp. 142–145, 2017.

[13] C. Carugno, C. Iacobellis, and G. Pedini, "Baropodometric studies in patients submitted to Grice-Green operation for primary valgus pronated flat foot," *Ital. J. Orthop. Traumatol.*, vol. 16, pp. 379–385, 1990.

[14] Kim, K.N., Lee, J.P., Lee, S.H., Lee, S.C. and Baik, J.M., 2016. Ergonomically designed replaceable and multifunctional triboelectric nanogenerator for a uniform contact. RSC Advances, 6(91), pp.88526-88530.

[15] Lin, Z., Wu, Z., Zhang, B., Wang, Y.C., Guo, H., Liu, G., Chen, C., Chen, Y., Yang, J. and Wang, Z.L., 2019. A triboelectric nanogenerator-based smart insole for multifunctional gait monitoring. Advanced Materials Technologies, 4(2), p.1800360.

[16] Mao, Y., Zhu, Y., Zhao, T., Jia, C., Wang, X. and Wang, Q., 2021. Portable mobile gait monitor system based on triboelectric nanogenerator for monitoring gait and powering electronics. Energies, 14(16), p.4996.

[17] Donyaparastlivari, L., Atmeh, M., Indic, P. and Ibrahim, A., 2023, April. A feasibility analysis of triboelectric energy harvester for hip implants. In 2023 IEEE 16th Dallas Circuits and Systems Conference (DCAS) (pp. 1-4). IEEE.

[18] Abumarar, Hadeel, and Alwathiqbellah Ibrahim. "A nonlinear impact-driven triboelectric vibration energy harvester for frequency up-conversion." Micromachines 14.5 (2023): 1082.

[19] Abumarar, Hadeel, Alwathiqbellah Ibrahim, and Abdallah Ramini. "Theoretical investigation of bistable piezoelectric energy harvester using frequency down-conversion." Active and Passive Smart Structures and Integrated Systems XVII. Vol. 12483. SPIE, 2023.